Optimal Force–Time Integral for Pulmonary Vein Isolation According to Anatomical Wall Thickness Under the Ablation Line

Akio Chikata, MD; Takeshi Kato, MD, PhD; Satoru Sakagami, MD, PhD; Chieko Kato, MD, PhD; Takahiro Saeki, MD, PhD; Keiichi Kawai, MD; Shin-ichiro Takashima, MD, PhD; Hisayoshi Murai, MD, PhD; Soichiro Usui, MD, PhD; Hiroshi Furusho, MD, PhD; Shuichi Kaneko, MD, PhD; Masayuki Takamura, MD, PhD

Background—Low contact force and force–time integral (FTI) during catheter ablation are associated with ineffective lesion formation, whereas excessively high contact force and FTI may increase the risk of complications. We sought to evaluate the optimal FTI for pulmonary vein (PV) isolation based on atrial wall thickness under the ablation line.

Methods and Results—Contact force parameters and FTI during anatomical ipsilateral PV isolation for atrial fibrillation and atrial wall thickness were assessed retrospectively in 59 consecutive patients for their first PV isolation procedure. The PV antrum was divided into 8 segments, and the wall thickness of each segment under the ablation line was determined using multidetector computed tomography. The FTI for each ablation point was divided by the wall thickness of the PV antrum segment where each point was located to obtain FTI/wall thickness. In total, 5335 radiofrequency applications were delivered, and 85 gaps in PV isolation ablation lines and 15 dormant conductions induced by adenosine were detected. The gaps or dormant conductions were significantly associated with low contact force, radiofrequency duration, FTI, and FTI/wall thickness. Among them, FTI/wall thickness had the best prediction value for gaps or dormant conductions by receiver operating characteristic curve analysis. FTI/ wall thickness of <76.4 gram-seconds per millimeter (gs/mm) predicted gaps or dormant conductions with sensitivity (88.0%) and specificity (83.6%), and FTI/wall thickness of <101.1 gs/mm was highly predictive (sensitivity 97.0%; specificity 69.6%).

Conclusions—FTI/wall thickness is a strong predictor of gap and dormant conduction formation in PV isolation. An FTI/wall thickness ≈100 gs/mm could be a suitable target for effective ablation. (*J Am Heart Assoc.* 2016;5:e003155 doi: 10.1161/ JAHA.115.003155)

Key Words: atrial fibrillation • atrial wall thickness • contact force • force–time integral • pulmonary vein isolation

R ecent progress and technical advances in catheter ablation have dramatically improved the success rate and safety of pulmonary vein isolation (PVI) for atrial fibrillation (AF). Real-time monitoring of tip-to-tissue contact force (CF) is a useful technique for confirming that the ablation electrode is applying appropriate pressure. The development of CF has allowed control of the quality of

lesions during radiofrequency (RF) ablation.[1,2] A low CF during catheter ablation is associated with ineffective lesion formation, whereas excessively high CF may result in an increased risk of steam pop, thrombus formation, or cardiac perforation,[3] particularly an atrioesophageal fistula in the posterior wall.[4] A recent study reported that CF and the force–time integral (FTI) during RF ablation are predictors of transmural lesion, with the best cutoff FTI value of >392 gram-seconds (gs).[5] The EFFICAS I study reported that ablation with a minimum FTI of <400 gs showed an increased likelihood of reconnection and that gap occurrence showed a strong trend with lower average CF and average FTI[6]; however, the left atrial (LA) wall under the catheter ablation line is not of uniform thickness, and it can be particularly thick in the left lateral ridge (LLR). Although the LLR does not only compose the myocardial fiber,[7] it has been reported that LLR thickness is associated with the recurrence of AF after PVI.[8]

For these reasons, we speculated that the optimal CF parameters for each lesion may differ according to the anatomical site and atrial wall thickness. The aim of this study was to evaluate the optimal CF or FTI for anatomical ipsilateral

PVI based on LA wall thickness under the catheter ablation line.

Methods

The study participants were 59 consecutive patients (118 ipsilateral veins) with symptomatic drug-refractory AF who were referred to our hospital between September 2014 and August 2015 for RF catheter ablation for their first procedure. We included patients who underwent anatomical ipsilateral PVI and who were assessed for dormant conduction (DC) by an intravenous bolus of adenosine.

The study was approved by the ethics committee at the National Hospital Organization, Kanazawa Medical Center. All patients gave written informed consent before the procedure. The PVI was performed in patients who anticoagulated effectively. Prior to the procedure, LA thrombus was excluded using laboratory data and cardiac computed tomography (CT) angiogram or transesophageal echocardiogram. Antiarrhythmic agents were discontinued before the procedure, allowing a washout period of 5 half-lives, although atrioventricular blocking agents were permitted in symptomatic patients. We excluded cases that required RF application in carina other than the pulmonary vein (PV) antrum to achieve PV isolation.

PVI Procedure

PV antrum isolation was performed in all 59 patients. All procedures were performed under conscious sedation or general anesthesia. A multielectrode catheter was transvenously inserted and positioned in the coronary sinus. A 10F intracardiac echocardiography catheter (64-element, 5.5–10.0 MHz, Soundstar; Biosense Webster) was advanced into the right atrium. Three-dimensional ultrasound images of the left atrium and PVs were acquired and processed using the Carto 3 system (Biosense Webster). The reconstructed 3-dimensional CT data sets were merged with the 3-dimensional ultrasound–derived geometries. After a double transseptal puncture was performed under intracardiac ultrasound guidance, heparin was intravenously administered to maintain activated clotting time of >300 seconds. Through transseptal accesses, nonsteerable sheaths (SL0; St. Jude Medical, Inc) and steerable sheaths (Agilis; St. Jude Medical, Inc) were placed into the left atrium. The irrigated CF ablation catheter (Navistar ThermoCool SmartTouch; Biosense Webster) was advanced into the left atrium through a steerable sheath, and extensive encircling PVI was performed guided by the 3-dimensional ultrasound geometries and 3-dimensional merged CT images. The catheter operator was not blinded to the CF during ablation. Ablations were performed in a temperature-controlled mode with the temperature limited to

43°C and the power limited to 25 W in the posterior segments and 30 W in the other segments. Luminal esophageal temperature was monitored using a luminal esophageal temperature probe (SensiTherm; St. Jude Medical), and we considered a luminal esophageal temperature of >39°C as requiring cessation of ablation. The irrigation flow rate was set to 2 mL/min during mapping and 17–30 mL/min during ablation. Ablations were performed with continuous dragging or point by point except for the regions of the posterior wall where the esophagus makes contact. The operator's decision to move 1 site to the next ablation site was based mainly on electrogram abatement and luminal esophageal temperature increase. The circumferential isolation was first performed anatomically without the circular catheter (Lasso) or the 1-mm multielectrode–mapping catheter (Pentaray), using an exclusively anatomical approach. The RF application time at each site varied, and PV antrum isolation was verified (as the absence of any PV potential or LA potential in the antral ablation area) using the Lasso or Pentaray catheter and/or the ablation catheter electrograms.

CT Data Acquisition and Measurements of the Anatomical Wall Thickness of the Left Atrium and PVs Under the Catheter Ablation Lines

All examinations were performed using a 64-detector-row CT (multidetector CT [MDCT]) scanner (Brilliance CT 64; Philips Electronics). For the contrast-enhanced scan, 20–21 mg of iodine per kg/s of contrast medium were injected for 15–18 seconds followed by 20 mL saline. The scan was started with a delay of 11 seconds after the detection of contrast in the main pulmonary artery. The data acquisition window was set at 40% to 75% of the R-R interval. Volume data were reconstructed into axial images with a slice thickness of 0.9 mm and were transferred to a workstation for postprocessing (Ziostation2; Ziosoft, Inc). For each PV, we divided the PV antrum into 8 segments under the ablation line, and quantitative measurements for each region were performed, as reported previously.[8] At the LLR and the carina between the superior and inferior PVs, we used images orthogonal to each region. The transmural myocardial thicknesses of the LLR at the superior and inferior PV were each calculated as the mean of 2 measurements taken from 2 directions. The carina–ridge region was also measured from 2 directions, and the mean was calculated. When several branches were present on the same-side PV, we adopted the thickest value of the carina. The PV antrum was defined as the region consisting of a 10-mm space between the PV ostium and the left atrium. In the segments other than the LLR, we measured the wall thickness of the PV antrum estimated to be on the catheter ablation line, using sagittal section. All data sets

were independently analyzed by radiologists experienced in MDCT.

Evaluation of Acute Gaps and DCs

After ipsilateral anatomical PV antrum isolation, all PVs were mapped to detect ablation gaps of PV-to-left atrium conduction. In the absence of gaps, the presence of DCs was assessed in each vein with an intravenous administration of 20 mg adenosine. The positions where RF application resulted in a change of sequence or abolition of the PV potential were defined as gap sites. A DC was defined as the reappearance of PV conduction, demonstrated by associated PV spikes of >1 beat, as recorded by the circular catheter. The positions where RF application resulted in a change of sequence or the abolition of DC were defined as DC sites. When 1 gap or DC site included multiple ablation points with the smallest Vigi-tag (Biosense Webster), we counted all of these points as gaps or DCs.

Determination of the Optimal FTI for Each Segment According to Wall Thickness

Ablation points were assigned to each segment of the PV antrum where they were located. FTI, maximum CF, average CF, minimum CF, RF duration, and RF power were obtained for each ablation point. CF parameters were obtained using the smallest Vigi-tag size. When one ablation site overlapped to the next site, even with the smallest Vigi-tag size, the higher FTI site was selected as an ablation point. The FTI for each ablation point was divided by the wall thickness of the PV atrium segment where the ablation point was located to calculate the ablation FTI required for every 1 mm of wall thickness (FTI/wall thickness).

Statistical Analysis

Statistical analyses were conducted using GraphPad Prism (GraphPad Software). Data are reported as mean±SD. Data were compared using unpaired t tests. All tests were 2 sided, and $P<0.05$ was considered statistically significant. The predictive values of different thresholds of CF and FTI for gaps and DCs were assessed using sensitivity, specificity, and receiver operating characteristic (ROC) curve analysis.

Results

Baseline characteristics of the patients in this study are presented in Table 1. The mean LA diameter on transthoracic echocardiography was 38.5±5.3 mm. Of the 59 patients, 20 (33.9%) were shown during the CT scan to have AF. Complete

Table 1. Characteristics of the Study Population

Characteristic	Overall (n=59)	Range or Percentage
Age, y	66.9±9.9	41–82
Sex, male, n (%)	44	74.6
Height, cm	164.7±8.4	144.0–179.4
Body weight, kg	60.4±9.9	43.7–85.2
Body mass index	22.4±2.7	16.2–28.1
Antiarrhythmic agents, n (%)		
None	14	23.7
Na channel blocker	24	40.7
β-blocker	31	52.5
Amiodarone	1	1.7
Bepridil	5	8.5
Hypertension, n (%)	26	44.1
Diabetes mellitis, n (%)	7	11.9
Ischemic heart disease, n (%)	8	13.6
Congestive heart failure, n (%)	8	13.6
CHA_2DS_2-VASC, n (%)		
0	9	15.3
1	13	22.0
≧2	37	62.7
Left ventricular ejection fraction (%)	66.1±8.7	42.0–79.6
Left atrial diameter, mm	38.5±5.3	26.1–52.1
Paroximal AF, n (%)	48	81.4
AF rhythm during MDCT scanning, n (%)	20	33.9
BNP, pg/mL	89.6±89.8	9.3–408.9
eGFR Cockroft-Gault, mL/min	63.8±12.8	42.0–105.6
NOAC, n (%)	51	86.4%
RF application number (n)	90.4±14.2	64–125

AF indicates atrial fibrillation; BNP, B-type natriuretic peptide; eGFR, estimated glomerular filtration rate; MDCT, multidetector computed tomography; NOAC, non-vitamin K antagonist oral anticoagulants; RF, radiofrequency.

PVI was achieved in 23 patients (39%) after ablation of single continuous circular lesions around ipsilateral PVs. All targeted PVs (118 ipsilateral veins) were successfully isolated by the end of the procedures. A total of 5335 RF applications were delivered. An average RF application number was 90.4±14.2 points per patient. Gaps and DCs were detected at 85 and 15 points, respectively.

Myocardial Wall Thickness Measured Using MDCT Images

Myocardial wall thickness under the ablation line was measured using MDCT. As shown in Figure 1, the LLR was
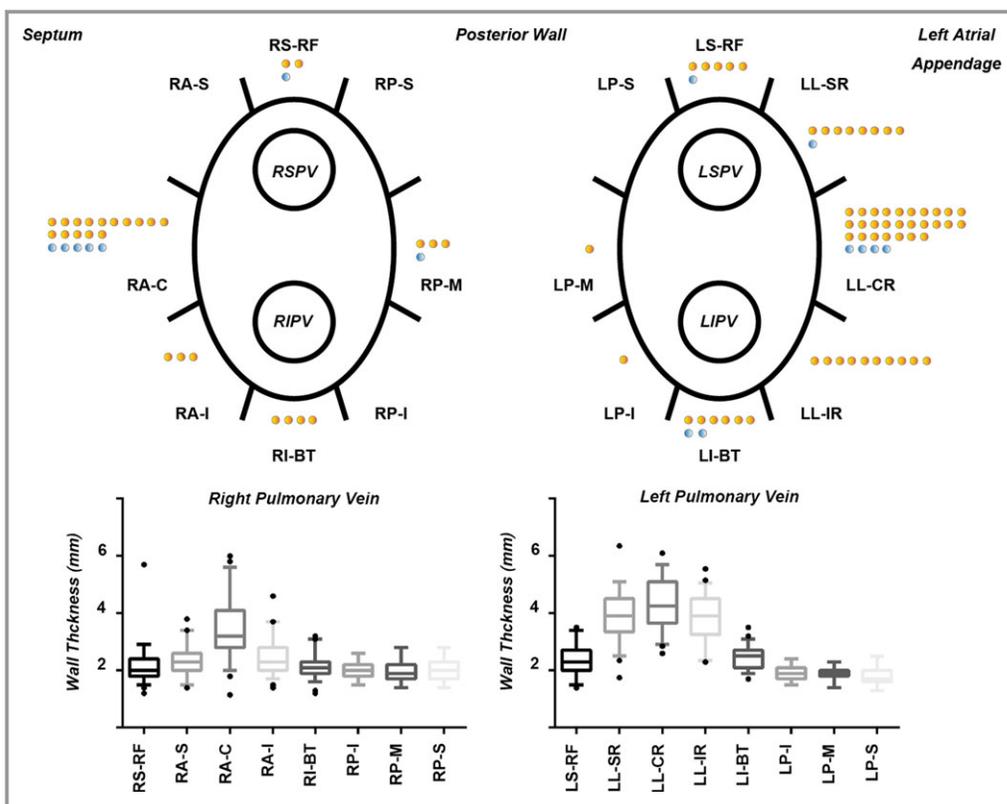
Figure 1. Myocardial thickness of each segment under the ablation line (lower panels) and distribution of acute gaps and dormant conductions (DCs) after pulmonary vein isolation (upper panels). Yellow circles represent acute gaps, blue circles represent DCs. LI-BT indicates left inferior bottom; LIPV, left inferior pulmonary vein; LL-CR, left lateral carina ridge; LL-IR, left lateral inferior ridge; LL-SR, left lateral superior ridge; LP-I, left posterior inferior; LP-M, left posterior middle; LP-S, left posterior superior; LSPV, left superior pulmonary vein; LS-RF, left superior roof; RA-C, right anterior carina; RA-I, right anterior inferior; RA-S, right anterior superior; RI-BT, right inferior bottom; RIPV, right inferior pulmonary vein; RP-I, right posterior inferior; RP-M, right posterior middle; RP-S, right posterior superior; RSPV, right superior pulmonary vein; RS-RF, right superior roof.

the thickest part of the ablation line, with mean thicknesses of 3.9±0.9 mm for the left lateral superior ridge, 3.9±0.8 mm for the left lateral inferior ridge, and 4.3±0.9 mm for the left lateral carina–ridge. The thinnest atrial wall was the left posterior wall (1.8±0.3 mm in the left posterior superior and 1.9±0.3 mm in the left posterior middle and the left posterior inferior). The wall thickness of each PV segment was not significantly affected by the presence of AF rhythm during CT scanning (Figure S1).

CF Parameters for Each Segment Under the Ablation Line

The CF parameters applied at each PV segment are shown in Table 2. The highest average CF (23.8±10.2 g) was applied to the right anterior inferior, and the lowest average CF was applied to the left lateral carina–ridge (15.8±6.2 g). The FTI was highest in the right anterior carina (538.7±377.8 gs). RF

duration time was the shortest and FTI was the lowest of all segments at the left posterior inferior (15.4±6.4 seconds and 234.7±100.0 gs, respectively) as a result of avoiding an increase in luminal esophageal temperature. FTI/wall thickness was higher in the anterior wall of the right PVs and lower in the LLR. The distribution of gaps and DCs was concentrated in the LLR and right anterior wall (Figure 1).

All CF parameters including CF, RF duration, FTI, and FTI/wall thickness were significantly lower in the lesions with gaps or DCs compared with the lesions without them. These correlations were similarly observed within each patient. The delivered RF power was not significantly different between the 2 groups (P=0.08) (Table 3).

Prediction of Gaps and DCs After PVI

ROC curves were made for FTI, average CF, maximum CF, RF duration, and FTI/wall thickness to determine the thresholds

Table 2. CF Parameters for Each Segment Under the Ablation Line

PV	Segment	Wall Thickness (mm)	Average CF (g)	Max CF (g)	Min CF (g)	RF Duration (s)	FTI (gs)	FTI/Wall Thickness (gs/mm)
Left	Superior roof	2.4±0.5	16.8±7.3	34.9±19.5	7.7±5.2	23.0±11.5	375.6±236.2	163.7±116.0
	Lateral superior ridge	3.9±0.9	16.7±6.9	32.6±16.7	6.2±4.8	26.4±13.8	434.9±299.4	114.2±77.9
	Lateral carina ridge	4.3±0.9	15.7±6.2	33.1±15.5	6.9±5.0	27.6±13.4	427.1±257.9	102.6±68.5
	Lateral inferior ridge	3.9±0.8	16.5±7.4	32.3±13.3	7.9±7.1	26.1±12.8	409.1±247.6	108.2±68.3
	Inferior bottom	2.5±0.4	17.7±8.0	31.3±11.6	8.4±7.5	20.2±10.6	333.5±209.2	136.4±87.7
	Posterior inferior	1.9±0.3	16.5±7.7	26.9±10.9	7.7±7.1	15.4±6.4	234.7±100.0	124.0±57.0
	Posterior middle	1.9±0.3	16.3±7.4	28.0±12.0	7.5±6.5	17.4±7.1	275.4±174.8	146.1±96.1
	Posterior superior	1.8±0.3	17.4±8.0	32.5±17.4	8.4±6.4	19.8±9.2	322.1±169.3	186.9±102.5
Right	Superior roof	2.1±0.6	21.2±8.4	58.7±27.9	6.8±6.1	19.7±9.6	397.9±216.7	190.9±110.5
	Anterior superior	2.3±0.5	19.9±8.4	35.3±13.5	9.2±7.1	22.8±10.7	436.4±275.6	191.2±119.7
	Anterior carina	3.4±1.1	22.2±10.4	35.6±13.6	9.8±8.6	25.3±13.5	538.7±377.8	164.3±122.6
	Anterior inferior	2.4±0.6	23.8±10.2	39.8±14.2	10.1±9.1	23.1±11.7	533.4±330.8	229.2±148.9
	Inferior bottom	2.1±0.4	23.4±10.9	41.1±15.0	7.8±9.4	20.2±9.6	448.3±270.7	205.1±111.4
	Posterior inferior	2.0±0.3	18.9±9.1	37.4±15.1	4.9±6.8	20.1±10.1	346.9±18.0	175.2±93.2
	Posterior middle	2.0±0.4	20.0±8.9	42.0±18.7	6.7±6.8	19.9±8.9	376.5±203.3	193.1±109.5
	Posterior superior	2.1±0.5	20.7±7.4	56.1±23.1	6.2±6.1	19.9±10.3	386.3±207.2	192.3±108.5

CF indicates contact force; FTI, force–time integral; gs, gram-seconds; Max, maximum; Min, minimum; PV, pulmonary vein; RF, radiofrequency.
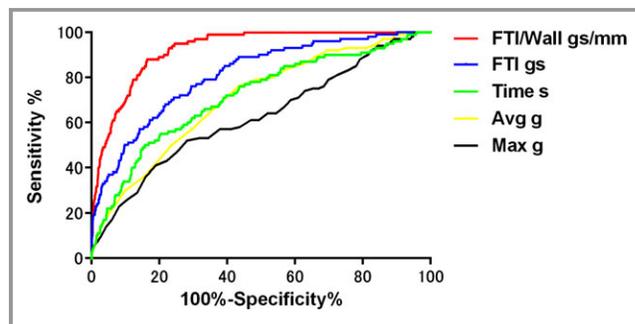
that best predict gaps or DCs (Figure 2). FTI/wall thickness showed the best prediction value with an area under the curve of 0.9242 (95% CI 0.9060–0.9425). The areas under the curve for FTI, average CF, maximum CF, and RF duration were 0.8101, 0.7046, 0.6246, and 0.7161, respectively. The best threshold for predicting gaps or DCs, defined by the position on the ROC curve at the minimum distance from the left corner of the ROC space, was an FTI/wall thickness of 76.4 gs/mm (sensitivity 88.0%; specificity 83.6%). An FTI/wall thickness of <101.1 gs/mm was highly predictive of gaps or DCs (sensitivity 97.0%; specificity 69.6%). An FTI/wall

thickness of <127.3 gs/mm predicted gaps or DCs with 100% sensitivity (specificity 55.01%). Conversely, an FTI of <475.5 gs showed high sensitivity but low specificity (sensitivity 97.0%; specificity 26.6%). Subgroup analysis revealed that FTI/wall thickness also showed the best prediction value

Table 3. Ablation Parameters at Each Point With a Gap or DC Compared With Those Without

	With Gap or DC (n=100)	Without Gap or DC (n=5235)	*P* Value
FTI, gs	199.0±12.3	407.9±3.7	<0.0001
Average CF, g	13.8±0.6	19.2±0.1	<0.0001
Max CF, g	30.4±1.5	37.6±0.3	0.0001
Minimum CF, g	5.3±0.5	7.6±0.1	0.0007
RF duration, s	15.2±0.9	22.46±0.2	<0.0001
FTI/wall thickness, gs/mm	50.6±2.4	164.8±1.5	<0.0001
RF power, W	28.7±0.2	28.0±0.1	0.08

CF indicates contact force; DC, dormant conduction; FTI, force–time integral; gs, gram-seconds; RF, radiofrequency.

Figure 2. Receiver operating characteristic curve analysis for acute gap and dormant conduction (DC) predictability. FTI/wall thickness showed the best prediction value with an area under the curve (AUC) of 0.9242 (95% CI 0.9060–0.9425, *P*<0.001 vs AUCs of FTI and the other contact force [CF] parameters). FTI, average CF, maximum CF, and RF duration had AUCs of 0.8101, 0.7046, 0.6246, and 0.7161, respectively. The best threshold for FTI/wall thickness for predicting acute gaps or DCs was 76.4 gs/mm (sensitivity 88.0%; specificity 83.6%). An FTI/wall thickness of <101.1 gs/mm was highly predictive of acute gap or DC (sensitivity 97.0%; specificity 69.6%). Avg indicates average; FTI, force–time integral; gs, gram-seconds; Max, maximum.

with an area under the curve in the patients whose CT scan was obtained during AF rhythm (Figure S2).

Discussion

We evaluated the utility of an optimal value for FTI in relation to the wall thickness under the PVI ablation line to predict gaps or DCs. Our major findings were as follows: (1) MDCT analysis revealed that the wall thickness was different at each part of the ablation line and was thickest at the LLR; (2) the gaps or DCs were significantly associated with low CF, RF duration, FTI, and FTI/wall thickness; and (3) ROC curve analysis identified FTI/wall thickness as the best predictor for gaps and DCs.

In this study, the wall thicknesses of the LLR, the right anterior carina, and the posterior walls were ≈4, 3.4, and <2 mm, respectively. These results are generally consistent with previous reports regarding Japanese patients.[8] In European studies using heart specimens by dissection and histological sections or by magnetic resonance angiography, the mean width of the LLR was greater.[7,9] Although the modalities used to measure wall thickness in those studies differed from ours, the different width may be related to race, age, or sex.

A lower average CF has been reported as a strong predictor of gap formation.[6,10,11] It has been reported that CF at the LLR tends to be low[12] and that the majority of conduction gaps after single continuous circular lesions around ipsilateral PVs were located at the LLR and the anterior wall of the right PV.[13] In the present study, the CF for the LLR was low, and most of the gaps and DCs were located at the LLR or the right anterior carina, which was consistent with previous reports.[12,13] We speculate that the lower CF and insufficient FTI against the thick atrial walls at the LLR and anterior right PV wall led to the formation of gaps and DCs. Although RF power is a known predictor of lesion size,[3,14–16] it had no significant impact on gap or DC formation in this study. This result might be derived from the fixed power output setting, which is uniform across the ablation line (25 W in posterior wall segments and 30 W in the other segments). Further study is required to test whether the addition of a power output parameter improves prediction performance of FTI/wall thickness.

It has been reported that a minimum FTI of ≈400 gs for each lesion was necessary to avoid reconnection[6,10] or to create transmural lesions in PVI.[5] Conversely, the relationship between FTI and electrogram attenuation plateaued at ≈500 gs, and FTI and impedance drop also plateaued at ≈500 gs.[17] Beyond this plateau point, continuation of ablation is unlikely to produce further gains but may increase the potential risk of complications such as perforation, steam pops, or damage to extracardiac structures.[17] Nevertheless, these studies did not take wall thickness into account, and it differs at each ablation point. In the present study, most of the gaps or DCs were concentrated at the LLR and the right anterior carina regardless of high FTI. Conversely, few gaps or DCs were observed at the posterior walls, where FTI were relatively low. These observations imply that FTI sufficient for creating transmural legions is higher for the thicker wall. Conversely, excess FTI for thin walls may bring a potential risk of damage to extracardiac structures such as the esophagus at the posterior wall of the LPV.

In this study, an average RF application number was ≈90 points per patient. Considering that even a few remaining gaps or DCs from these ablation points can lead to AF recurrence, more sensitive FTI/wall thickness values should be targeted to avoid formation of gaps and DCs. Although FTI/wall thickness of >76.4 gs/mm has a best predictive value on the basis of ROC analysis, with the best balance between sensitivity and specificity, FTI/wall thickness of 101.1 gs/mm with higher sensitivity could be a more suitable target to avoid formation of gaps and DCs.

Study Limitations

First, this study was a single-center retrospective study with a relatively small number of patients. Our participants were relatively old Japanese patients with small physiques, and it is not known whether the present results would be applicable to other races. Second, our measurements of wall thickness were made on the basis of the assumed ablation lines on MDCT data and might not match the actual ablation line. In addition, the AF rhythm observed in 33.9% of the patients during CT scanning may have affected the quality of CT images and the measurements of wall thickness. Third, the number of gaps and DCs observed in the present study is greater than the number observed in the previous report[13]; however, complete PVI was achieved in 39% of the patients after ablation of single continuous circular lesions around ipsilateral PVs, which is consistent with the previous report. We suppose that the larger number of gaps and DCs was related to our definition. In this study, when 1 gap or DC site included multiple ablation points with the smallest Vigi-tag size, we counted all of these points as gaps or DCs. This might affect the value of optimal FTI. Finally, we evaluated the effect of FTI only on acute success and the elimination of DCs. Although it has been reported that the presence of DCs is associated with a higher risk of recurrence after PVI,[18] it is still unclear whether the higher FTI/wall thickness actually leads to the better outcome of AF ablation.

Conclusions

This study demonstrated that the optimal FTI for achieving effective ablation for ipsilateral anatomical PVI varies at each point along the ablation line. Atrial wall thickness is not

uniform under the ablation line, and FTI/wall thickness is a strong predictor of gap and DC formation. FTI/wall thickness ≈100 gs/mm could be a suitable target value to achieve effective ablation.

Disclosures

None.

References

1. Thiagalingam A, D'Avila A, Foley L, Guerrero JL, Lambert H, Leo G, Ruskin JN, Reddy VY. Importance of catheter contact force during irrigated radiofrequency ablation: evaluation in a porcine ex vivo model using a force-sensing catheter. *J Cardiovasc Electrophysiol*. 2010;21:806–811.

2. Okumura Y, Johnson SB, Bunch TJ, Henz BD, O'Brien CJ, Packer DL. A systematical analysis of in vivo contact forces on virtual catheter tip/tissue surface contact during cardiac mapping and intervention. *J Cardiovasc Electrophysiol*. 2008;19:632–640.

3. Yokoyama K, Nakagawa H, Shah DC, Lambert H, Leo G, Aeby N, Ikeda A, Pitha JV, Sharma T, Lazzara R, Jackman WM. Novel contact force sensor incorporated in irrigated radiofrequency ablation catheter predicts lesion size and incidence of steam pop and thrombus. *Circ Arrhythm Electrophysiol*. 2008;1:354–362.

4. Pappone C, Oral H, Santinelli V, Vicedomini G, Lang CC, Manguso F, Torracca L, Benussi S, Alfieri O, Hong R, Lau W, Hirata K, Shikuma N, Hall B, Morady F. Atrio-esophageal fistula as a complication of percutaneous transcatheter ablation of atrial fibrillation. *Circulation*. 2004;109:2724–2726.

5. Squara F, Latcu DG, Massaad Y, Mahjoub M, Bun SS, Saoudi N. Contact force and force-time integral in atrial radiofrequency ablation predict transmurality of lesions. *Europace*. 2014;16:660–667.

6. Neuzil P, Reddy VY, Kautzner J, Petru J, Wichterle D, Shah D, Lambert H, Yulzari A, Wissner E, Kuck KH. Electrical reconnection after pulmonary vein isolation is contingent on contact force during initial treatment: results from the EFFICAS I study. *Circ Arrhythm Electrophysiol*. 2013;6:327–333.

7. Cabrera JA, Ho SY, Climent V, Sanchez-Quintana D. The architecture of the left lateral atrial wall: a particular anatomic region with implications for ablation of atrial fibrillation. *Eur Heart J*. 2008;29:356–362.

8. Suenari K, Nakano Y, Hirai Y, Ogi H, Oda N, Makita Y, Ueda S, Kajihara K, Tokuyama T, Motoda C, Fujiwara M, Chayama K, Kihara Y. Left atrial thickness under the catheter ablation lines in patients with paroxysmal atrial fibrillation: insights from 64-slice multidetector computed tomography. *Heart Vessels*. 2013;28:360–368.

9. Schmidt B, Ernst S, Ouyang F, Chun KR, Broemel T, Bansch D, Kuck KH, Antz M. External and endoluminal analysis of left atrial anatomy and the pulmonary veins in three-dimensional reconstructions of magnetic resonance angiography: the full insight from inside. *J Cardiovasc Electrophysiol*. 2006;17:957–964.

10. Kautzner J, Neuzil P, Lambert H, Peichl P, Petru J, Cihak R, Skoda J, Wichterle D, Wissner E, Yulzari A, Kuck KH. EFFICAS II: optimization of catheter contact force improves outcome of pulmonary vein isolation for paroxysmal atrial fibrillation. *Europace*. 2015;17:1229–1235.

11. Reddy VY, Shah D, Kautzner J, Schmidt B, Saoudi N, Herrera C, Jais P, Hindricks G, Peichl P, Yulzari A, Lambert H, Neuzil P, Natale A, Kuck KH. The relationship between contact force and clinical outcome during radiofrequency catheter ablation of atrial fibrillation in the TOCCATA study. *Heart Rhythm*. 2012;9:1789–1795.

12. Schluermann F, Krauss T, Biermann J, Hartmann M, Trolese L, Pache G, Bode C, Asbach S. In vivo contact force measurements and correlation with left atrial anatomy during catheter ablation of atrial fibrillation. *Europace*. 2015;17:1526–1532.

13. Furnkranz A, Julian JK, Schmidt B, Wohlmuth P, Tilz R, Kuck KH, Ouyang F. Ipsilateral pulmonary vein isolation performed by a single continuous circular lesion: role of pulmonary vein mapping during ablation. *Europace*. 2011;13:935–941.

14. Wittkampf FH, Hauer RN, Robles de Medina EO. Control of radiofrequency lesion size by power regulation. *Circulation*. 1989;80:962–968.

15. Di Biase L, Natale A, Barrett C, Tan C, Elayi CS, Ching CK, Wang P, Al-Ahmad A, Arruda M, Burkhardt JD, Wisnoskey BJ, Chowdhury P, De Marco S, Armaganijan L, Litwak KN, Schweikert RA, Cummings JE. Relationship between catheter forces, lesion characteristics, "popping", and char formation: experience with robotic navigation system. *J Cardiovasc Electrophysiol*. 2009;20:436–440.

16. Shah DC, Lambert H, Nakagawa H, Langenkamp A, Aeby N, Leo G. Area under the real-time contact force curve (force-time integral) predicts radiofrequency lesion size in an in vitro contractile model. *J Cardiovasc Electrophysiol*. 2010;21:1038–1043.

17. Ullah W, Hunter RJ, Baker V, Dhinoja MB, Sporton S, Earley MJ, Schilling RJ. Target indices for clinical ablation in atrial fibrillation: insights from contact force, electrogram, and biophysical parameter analysis. *Circ Arrhythm Electrophysiol*. 2014;7:63–68.

18. Matsuo S, Yamane T, Date T, Inada K, Kanzaki Y, Tokuda M, Shibayama K, Miyanaga S, Miyazaki H, Sugimoto K, Mochizuki S. Reduction of AF recurrence after pulmonary vein isolation by eliminating ATP-induced transient venous reconduction. *J Cardiovasc Electrophysiol*. 2007;18:704–708.